AIAA JOURNAL
Vol. 46, No. 8, August 2008

Response of an Oscillating System to Harmonic Forces of Time-Varying Frequency

Grant M. Henson*
The Aerospace Corporation, El Segundo, California 90245

DOI: 10.2514/1.34662

Exact solutions for the steady-state response of a viscously damped linear system to excitations of sinusoidally varying frequency are presented. Solutions for the response to forces and base motions are derived, along with an expression for the root-mean-square response that does not require integration of the equation of motion. The solutions are used to calculate the response of a flexibly supported component to base motions and applied forces. It is shown that resonant response can occur even if the instantaneous excitation frequency never approaches the natural frequency. The dynamic attenuation for various rates of passage through resonance is calculated. Dependence of the response on system parameters is investigated. Finally, the response to a rotating unbalance with sinusoidally varying speed, such as may occur in turbomachinery under closed-loop speed control, is investigated. An exact but cumbersome solution valid for all speeds may be obtained. As a practicable alternative, it is shown that a force input may be constructed such that the exact solution to that simpler problem closely approximates the response to the unbalance. The approximation is valid when the rotational speed changes slowly compared with the period of the underlying oscillation.

Nomenclature

a	=	frequency parameter for linear sweep
b	=	frequency parameter for linear sweep
c	=	damping coefficient
F	=	excitation force amplitude
f	=	exact forcing function
f_{SA}	=	shake-approximation forcing function
g	=	dimensionless carrier frequency
h	=	modulation index
J_m	=	mth-order Bessel function of the first kind
$\tilde{J}_m$	=	Bessel function restricted to integral order
k	=	spring constant
M	=	moving mass
m	=	index in series solution
m_u	=	effective unbalance mass
p	=	dimensionless modulation frequency
q	=	frequency parameter in Lewis formulation
R	=	dimensionless displacement in Lewis formulation
r	=	effective unbalance radius
t	=	dimensional time
v	=	dummy variable in Jacobi–Anger expansion
x	=	dimensional displacement
y	=	dimensionless displacement
y_{rms}	=	dimensionless root-mean-square displacement
z	=	dimensionless time in Lewis formulation
ζ	=	damping ratio
θ	=	cosine argument in forcing function
λ	=	damping parameter in Lewis formulation
τ	=	dimensionless time
ϕ	=	dummy variable in Jacobi–Anger expansion
Ω_m	=	mth frequency parameter in steady-state solution
ω_n	=	undamped natural frequency

Presented as Paper 2358 at the 48th AIAA/ASME/AHS/ASC Structures, Structural Dynamics, and Materials Conference, Honolulu, HI, 23–26 April 2007; received 18 September 2007; revision received 11 February 2008; accepted for publication 11 February 2008.

*Currently Principal Engineer, Analex Corporation, 1000 Apollo Drive, Brook Park, Ohio 44142. Senior Member AIAA.

I. Introduction

ALTHOUGH most vibration analysis and much testing involves constant-frequency excitation, harmonic excitations with time-varying frequency are ubiquitous. Rotating machinery must start up and shut down, and even in nominally steady operation, it never maintains exactly the same speed. Continuous sine-sweep testing subjects the test piece to base motion of varying frequency.

A given excitation may be represented as a force or as a base motion, depending on which is more readily described. For instance, a building responding to an earthquake experiences forces and displacements at its foundation; the displacements are easily characterized by seismographs, whereas the forces are usually not available. In contrast, a load-controlled vibration test subjects the test article to known forces, but the accelerations may not be directly available. Forces and base motions may arise from longitudinal shaking or from rotation of unbalanced machinery.

Two cases of practical interest are a linearly varying frequency, perhaps representative of startup or shutdown of rotating machinery, and frequency that varies periodically, representative of, for example, unbalanced machinery with speed governed by a closed-loop controller. When the frequency varies linearly, the excitation is aperiodic, and the response is therefore essentially transient. However, when the frequency varies periodically, steady-state response may be calculated.

Significant work in this area has been limited to the case of linearly changing frequency. In an early, widely cited paper, Lewis [1] analyzed forces of linearly increasing or decreasing frequency with an ingenious, yet laborious, method for estimating the response envelope. More recently, Zhou and Shi [2] calculated the unbalance response of a Jeffcott rotor when its speed increases linearly. Markert and Seidler [3] reviewed the numerous approximation formulas in the literature for the peak response during a linear sweep. They also derived new formulas for the approximate peak response to various types of excitations, all having linearly varying frequency, based on an exact solution of a form different from that of Lewis [1]. Cronin [4] obtained perturbation solutions for force inputs with slowly, linearly changing frequency and also studied the response to exponentially increasing frequency. Furthermore, he obtained an exact solution for the response of an *undamped* system to a force input of sinusoidally varying frequency.

In the present paper, the linear-sweep force input is examined as an introduction to the important aspects of the problem, and the time history of the response is obtained by numerical integration. Then exact steady-state solutions for the damped response to forces and

base motions of sinusoidally varying frequency are derived, along with a compact representation of the root-mean-square (rms) response that does not require numerical integration of the equation of motion. No restrictions are placed on the system parameters. Finally, the rotating unbalance problem is addressed for cases where the rotational speed of the machinery varies sinusoidally with time, in particular, to investigate whether such excitations may be approximated with a force input.

II. Force Input of Linearly Varying Frequency

Consider a viscously damped single-degree-of-freedom (SDOF) oscillator excited by a harmonic force. Let the cosine argument of the force as a function of time t be $\theta(t)$. The equation of motion (EOM) is

$$\ddot{x} + 2\zeta\omega_n\dot{x} + \omega_n^2 x = \frac{F}{M}\cos\theta(t) \tag{1}$$

where F is the amplitude of the force, M is the sprung mass, ζ is the damping ratio, and ω_n is the undamped natural frequency. Adopting the variables $\tau \equiv \omega_n t$ and $y \equiv M\omega_n^2 x/F$, Eq. (1) takes the dimensionless form

$$y'' + 2\zeta y' + y = \cos\theta(\tau) \tag{2}$$

where prime denotes differentiation with respect to τ. When the force input is specified, the response $y(\tau)$ may be calculated straightforwardly by numerical integration. However, such an approach provides little insight and may be impractical for certain types of forcing functions.

Almost all steady-state deterministic analyses are limited to constant-frequency forcing functions. However, in this paper, the focus is on cases where frequency varies with time, which introduces some subtleties to the relationship between frequency and the cosine argument of the force. When the excitation frequency is constant, it is natural to write $\theta(\tau)$ as $\omega\tau$, where ω is the rate of change of the cosine argument. However, when the frequency changes with time, the physical interpretation of the coefficient of time as the rate of change of the cosine argument is no longer valid. Consider the case where the rate of change of the cosine argument changes linearly with time. The cosine argument for a linear frequency sweep starting from initial frequency a is

$$\theta(\tau) = a\tau + b\tau^2 \tag{3}$$

The resulting forcing function $\cos(a\tau + b\tau^2)$ has an instantaneous frequency that is a linear function of dimensionless time τ:

$$\frac{\mathrm{d}}{\mathrm{d}\tau}(a\tau + b\tau^2) = a + 2b\tau \tag{4}$$

and so $2b$ may be interpreted as the sweep rate. In contrast to the constant-frequency case, the cosine argument is not equal to frequency times time (which would be the meaningless expression $a\tau + 2b\tau^2$), but rather is equal to the *integral* of the cosine argument with respect to time.

Inserting expression (3) for the cosine argument into the EOM (2) yields

$$y'' + 2\zeta y' + y = \cos(a\tau + b\tau^2) \tag{5}$$

which represents a case of time-varying frequency that is easily stated, but difficult to analyze, due to its aperiodicity. Even for this simple case, the response involves integrals that cannot be evaluated in closed form. Lewis considered this problem in a widely cited paper from 1932 [1]. He remarked, regarding direct numerical integration of the response,

> In cases of engineering interest, involving relatively slow acceleration rates, there may be several hundred nearly equal positive and negative loops in the integrand between time zero and the critical speed. For this reason we consider their evaluation, with the slightest attempt at accuracy, quite impossible by any direct method of numerical integration, or by mechanical or electrical integraphs.

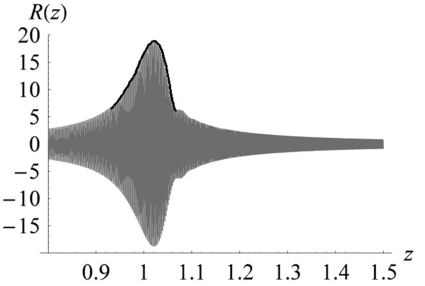

Fig. 1 Numerical integration (gray) compared with the solution envelope for Eq. (6) calculated by Lewis (black) for $q = 424$ and $\lambda = 0.3$.

In modern parlance, the problem is stiff. The situation can in fact be somewhat more challenging than Lewis [1] anticipated. Resonant frequencies typical of higher modes of light- or hard-mounted components can result in ten thousand or more cycles during a time interval long enough to capture the steady-state response. The time step must be small enough to adequately resolve each cycle, and it may be necessary to evaluate complicated functions at each step. Accurate analysis of realistic situations by numerical integration is within the capabilities of a modern workstation, but not comfortably so.

Using an approximation method involving contour integration, Lewis [1] obtained numerical solutions for the envelope (not the complete time history) of the solution to the EOM.

$$\frac{\mathrm{d}^2R}{\mathrm{d}z^2} + 2\sqrt{\frac{\pi q}{\lambda}}\frac{\mathrm{d}R}{\mathrm{d}z} + 4\pi^2q^2R = 4\pi^2q^2\cos\pi qz^2 \tag{6}$$

Equation (6) is the same as Eq. (5) with $a = 0$ and the parameters from the two forms related by

$$z \equiv 2b\tau \qquad R \equiv y \qquad q \equiv \frac{1}{4\pi b} \qquad \lambda \equiv \frac{b}{\zeta^2} \tag{7}$$

Figure 1 shows that the numerical solution for $q = 424$ and $\lambda = 0.3$ is in agreement with Lewis's [1] envelope (these parameter values were chosen to match those used by Lewis). The numerical solutions appearing in the present paper were obtained using a commercial implementation of the LSODA code, which automatically selects between a nonstiff Adams method and a stiff Gear backward differentiation method during the solution [5].

III. Force Input of Sinusoidally Varying Frequency

A. Theoretical Development

Returning to the dimensionless EOM (2), consider a harmonic excitation with a frequency that varies sinusoidally with time, as $\omega(\tau) = g + ph\cos p\tau$. Then the forcing function is

$$f(\tau) \equiv \cos\theta(\tau) = \cos\left(\int_0^\tau \omega(\tau^*)\,\mathrm{d}\tau^*\right) = \cos(g\tau + h\sin p\tau) \tag{8}$$

Function (8) is a frequency-modulated signal. Figure 2 shows an example of this type of signal. We refer to g as the carrier frequency, p as the modulation frequency, and h as the modulation index, taking this terminology from the study of frequency-modulated signals in

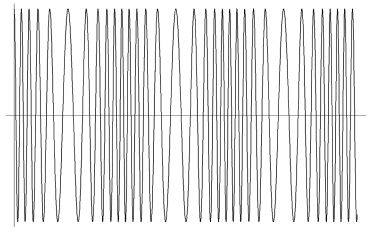

Fig. 2 A frequency-modulated signal.

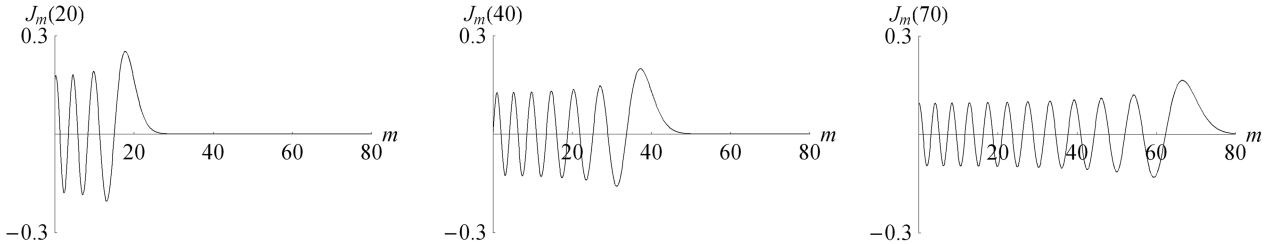

a) Argument of 20 **b) Argument of 40** **c) Argument of 70**

Fig. 3 Bessel functions for large argument and order, plotted as a function of order.

communications theory[†] (see, for example, Sturley [6]). These are all dimensionless quantities in the present formulation. Typical problems of interest involve small variations in frequency near a resonant peak; for these conditions, g will be close to 1 and p will be small compared with 1. The parameters may, however, take any real values.[‡] In particular, the frequency may change on a time scale comparable with the period of the underlying oscillation.

To use existing solutions from linear systems theory, the iterated trigonometric function in Eq. (8) must be "unraveled." First, the forcing function is rewritten, using a trigonometric identity, as

$$f(\tau) \equiv \cos g\tau \cos(h \sin p\tau) - \sin g\tau \sin(h \sin p\tau) \tag{9}$$

Using the Jacobi–Anger expansion (see, for example, Cantrell [7]),

$$e^{iv\cos\phi} = \sum_{m=-\infty}^{\infty} i^m J_m(v) e^{im\phi} \tag{10}$$

where $J_m(\cdot)$ is the mth-order Bessel function of the first kind, it can be shown that

$$\begin{aligned} \cos(h \sin p\tau) &= \sum_{m=-\infty}^{\infty} J_m(h) \cos mp\tau \quad \text{and} \\ \sin(h \sin p\tau) &= \sum_{m=-\infty}^{\infty} J_m(h) \sin mp\tau \end{aligned} \tag{11}$$

Then

$$\begin{aligned} f(\tau) &= \cos g\tau \sum_{m=-\infty}^{\infty} J_m(h) \cos mp\tau - \sin g\tau \sum_{m=-\infty}^{\infty} J_m(h) \sin mp\tau \\ &= \sum_{m=-\infty}^{\infty} J_m(h) \cos(g\tau + mp\tau) \end{aligned} \tag{12}$$

Now the EOM can be written

$$y'' + 2\zeta y' + y = \sum_{m=-\infty}^{\infty} J_m(h) \cos \Omega_m \tau \tag{13}$$

where $\Omega_m \equiv g + mp$. The steady-state response is

$$y(\tau) = \sum_{m=-\infty}^{\infty} J_m(h) \frac{\left(1 - \Omega_m^2\right) \cos \Omega_m \tau + 2\zeta\Omega_m \sin \Omega_m \tau}{\Omega_m^4 + 2\left(2\zeta^2 - 1\right)\Omega_m^2 + 1} \tag{14}$$

This is the exact steady-state solution to the problem. If the peak steady-state response is of interest, Eq. (14) can be evaluated and plotted over about one period of the modulation frequency, and the peak can be found from the response curve, or an envelope function can be constructed and maximized. However, for a fatigue assessment of an excited component, the rms response is often more useful. Using Parseval's formula, the mean-square response is

$$y_{\text{rms}}^2 = \tilde{J}_{-g/p}^2(h) + \frac{1}{2} \sum_{\substack{m=-\infty \\ m \neq -g/p}}^{\infty} \frac{J_m^2(h)}{\left(1 - \Omega_m^2\right)^2 + (2\zeta\Omega_m)^2} \tag{15}$$

where

$$\tilde{J}_m(\cdot) = \begin{cases} J_m(\cdot) & \text{if } m \text{ is a integer} \\ 0 & \text{otherwise} \end{cases} \tag{16}$$

Function (16), which is discontinuous, is discussed further in Appendix A. Equation (15) may be used to calculate the rms response without evaluating Eq. (14) or resorting to numerical integration. The peculiar exception $m = -g/p$, corresponding to zero frequency, is separated from the sum because it does not carry the factor of $\frac{1}{2}$ in Parseval's formula. Because m is an integer, this term only exists for forcing functions with g exactly an integral multiple of p and is insignificant when, as is usually the case, $g/p > h$. See Appendix A for more discussion of the zero-frequency term.

When no damping is present, the solution simplifies to

$$y(\tau) = \sum_{m=-\infty}^{\infty} \frac{J_m(h) \cos \Omega_m \tau}{1 - \Omega_m^2} \tag{17}$$

This special case was obtained in a different form by Cronin [4], which was the only other exact treatment of nonlinear frequency sweeping found in the open literature.

The convergence rates of the series expressions (14) and (15) are governed by the asymptotic behavior of the Bessel function for large-order m. Figure 3 shows that the mth-order Bessel function dies out for arguments a little larger than m. Therefore, results within engineering accuracy may be expected when $\text{int}(h)$ terms on each side of the series are retained, for a total of $2\,\text{int}(h) + 1$ terms. For large values of h, calculation of the complete time history via Eq. (14) may become impractical, but an accurate estimate of the rms response can always be computed quickly using Eq. (15). Convergence is discussed in more detail in Sec. III.B.

Unbounded response occurs when the denominator in Eq. (15) vanishes. This can only happen when damping is zero and any of the infinite set of conditions

$$\Omega_m \equiv g + mp = \pm 1 \qquad m = 0, \pm 1, \pm 2 \ldots \tag{18}$$

are satisfied. Included in this set of conditions is $g = 1$, where the oscillating frequency is centered about the natural frequency. If g and p do not satisfy any of the conditions (18), then the response remains bounded even if the undamped natural frequency is traversed repeatedly.

Conversely, it is possible for unbounded response to occur even if the instantaneous excitation frequency never approaches the undamped natural frequency. For example, with $g = 0.8$, $p = 0.04$, and $h = 1$, the excitation frequency never exceeds 0.84, which is 16% lower than the undamped natural frequency. But $g + mp = 1$ for $m = 5$, and so the response of an undamped system would be unbounded. When damping exists, the response would be large, perhaps destructively so, but bounded.

[†]In communications theory, forcing functions of this type have been extensively studied, with emphasis on the properties of the signal itself and demodulation methods rather than on the time-domain response of the various linear systems considered here.

[‡]Function (8) can, additionally, represent excitations that are interesting and realistic but not readily identifiable as dithering sinusoids (see Appendix A). The solutions presented in this paper are valid for any real values of g, h, and p.

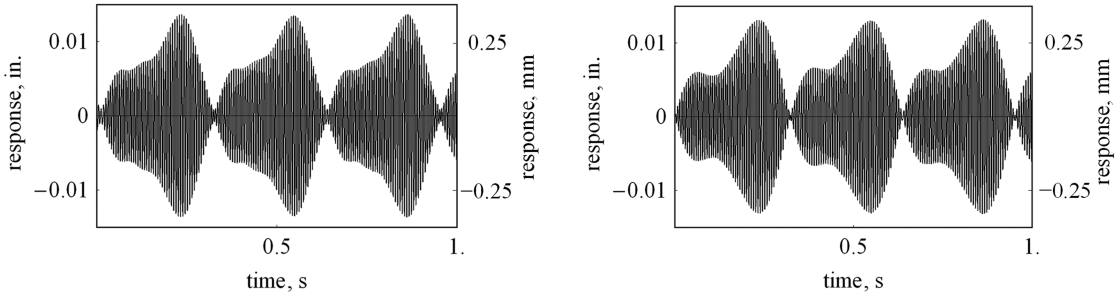

a) Steady-state response via exact solution truncated to $m_{max} = 5$

b) Complete response via numerical integration

Fig. 4 Response of a component with natural frequency 1000 rad/s (159 Hz) to a harmonic force varying sinusoidally between 950 rad/s (151 Hz) and 1050 rad/s (167 Hz). The truncated exact solution (14) and the numerically integrated solution are very close.

B. Component Response to Force of Sinusoidally Varying Frequency

Consider a 1-lbm (0.454-kg) component with a natural frequency of 1000 rad/s (159 Hz) excited by a harmonic force of amplitude 1 lb (4.45 N). The forcing frequency varies sinusoidally from 950 rad/s circular (151 Hz) to 1050 rad/s circular (167 Hz) and back 10 times in every 2π s. The system damping is 1% of critical: $\zeta = 0.01$.

The forcing function is

$$\cos\theta(t) = \cos(1000t + 5\sin 10t) = \cos(\tau + 5\sin 0.01\tau) \quad (19)$$

where the dimensionless time is $\tau = 1000t$. Thus, $g = 1$, $p = 0.01$, and $h = 5$. The steady-state response, calculated from the exact series solution (14) truncated to $m_{max} = 5$, is shown in Fig. 4a. The complete response, obtained by numerical integration with the initial conditions $y(0) = 0$ and $y'(0) = 0$, is shown for comparison in Fig. 4b. The peak dimensionless response is 0.0131 in. (0.332 mm), which is 68% of the amplitude of 0.0193 in. (0.490 mm) for sine dwell at the undamped natural frequency. The rms response, calculated from Eq. (15), is 0.0084 in. (0.213 mm).

The exact series solution truncated to $m_{max} = 5$ (Fig. 4a) differs slightly from the numerical solution (Fig. 4b), with the difference being most pronounced around $t = 0.15$ s. To examine the convergence of the closed-form solution, the calculated rms and peak values are plotted as more and more terms are retained in the sum (Fig. 5). Convergence is not monotonic. The calculated rms value is within 0.3% of the converged value with $m_{max} = h = 5$ (that is, with 11 terms retained in the sum). The calculated peak response is within 4% of the peak value from numerical integration with $m_{max} = 5$ and within 0.5% with $m_{max} = 7$. So the rule of thumb $m_{max} = \text{int}(h)$ works well in this case, judging by the convergence of the rms and peak responses. If accuracy over the *entire* time history is required, it may be necessary to sum a few more terms.

C. Parameter Studies

Parameter studies are now presented to demonstrate the sensitivity of the response to changes in the system parameters g, p, h, and ζ. Most cases of practical interest will involve frequencies that cross or at least approach the natural frequency of the excited component. Thus, the dimensionless carrier frequency g will be roughly between 0.8 and 1.2. The modulation frequency p will usually be much smaller than the carrier frequency. The scaled rms response $2\sqrt{2}\zeta y_{rms}$, which equals unity for sine dwell at the undamped natural frequency, is plotted. Thus, these plots illustrate the "dynamic attenuation" of the steady-state rms response. Note that because the scaling involves the damping ratio ζ, the scale factor is different for each curve. This accounts for the fact that the scaled response is generally higher as damping increases. The unscaled response is, of course, lower for higher damping. To dispense with any concerns about convergence, the sum is carried to $m_{max} = 70$ for the studied values $0 \le h \le 50$.

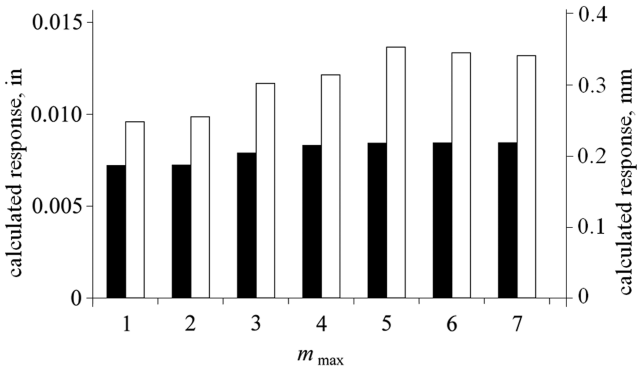

Fig. 5 Convergence of the peak response (white bars) and rms response (dark bars) as more and more terms are retained in the series expression (15). The total number of terms is $2m_{max} + 1$.

First, the effect of the modulation index h on the response is studied. The modulation index is a measure of the deviation of the frequency from its mean value; that is, it is proportional to the amplitude of the sinusoidal plot of frequency versus time. Figure 6a shows the scaled rms response as a function of h for $g = 1$ and $p = 0.01$ and three different values of ζ: 0.001, which represents a very lightly damped component, 0.01, which is a typical damping value for a structure, and 0.1, which suggests the presence of intentional damping. The response is generally attenuated more for larger values of h, although the attenuation oscillates, particularly when damping is light. Also, the less damping there is in the system, the more the response is dynamically attenuated. All three curves meet at a value of 1 for $h = 0$, which represents constant-frequency excitation. It is concluded that the dynamic attenuation associated with sinusoidal "dithering" of the excitation frequency is, in general, a strongly nonlinear function of the system parameters.

The set of conditions (18) show that for the parameter values $g = 1$ and $p = 0.01$ used to generate Fig. 6a, but with zero damping, the $m = 0$ and -200 terms in the sum become unbounded. However, the fact that the $m = -200$ term is unbounded for zero damping does not mean it is ever significant for realistically damped cases. The coefficient $J_{-200}(h)$ is so small that for any realistic damping level, the $m = -200$ term never contributes significantly to the response. The rule of thumb that terms beyond $m = \pm\text{int}(h)$ may be truncated is still valid. But as it is only a rule of thumb, it should be used cautiously.

Figure 6b shows the influence of h for a fixed value of damping $\zeta = 0.01$ and three values of the modulating frequency p. The response is again attenuated more for larger values of h. For the largest value of the modulation frequency ($p = 0.2$), the dimensionless frequency deviation ph exceeds 1.0 for $h > 5$. In this range, negative instantaneous frequencies occur (in the sense that $\omega(\tau) = g + ph\cos p\tau$ takes on negative values for some τ) and the excitation loses its sinusoidal appearance. The attenuation wanders irregularly from the oscillating trend seen in the other plotted curves.

IV. Base Motion of Sinusoidally Varying Frequency

A. Theoretical Development

Markert and Seidler [3], among others, have discussed the difference between a force input, a base motion, and an unbalance

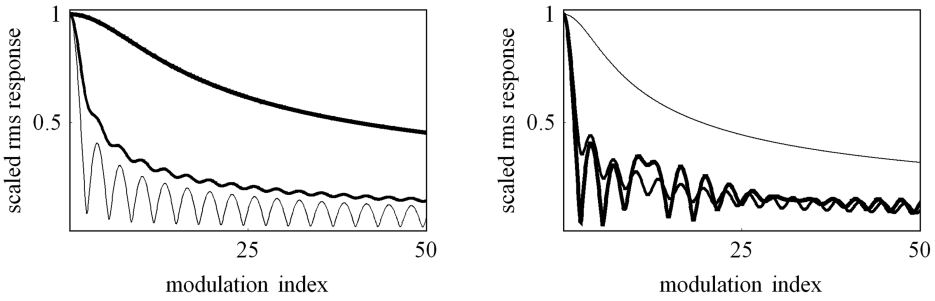

a) $\zeta = 0.001$ (thin line), $\zeta = 0.01$ (medium line), and $\zeta = 0.1$ (thick line); $g = 1$ for all curves

b) $p = 0.002$ (thin line), $p = 0.02$ (medium line), and $p = 0.2$ (thick line); $\zeta = 0.01$ for all curves

Fig. 6 Effect of the dimensionless modulation index h on the response to a force input of sinusoidally varying frequency.

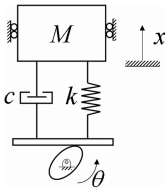

Fig. 7 A SDOF system subjected to harmonic base motion.

excitation with attention to time-varying frequencies. In this section, exact solutions are derived for the response of a structure in absolute coordinates to a base motion of sinusoidally varying frequency. (Rotating unbalance is considered in Sec. V.) The mechanical model is shown in Fig. 7. Using the same dimensionless variables as in the previous section, except that now $y \equiv x/Y$, where Y is the base motion amplitude, and the EOM is

$$y'' + 2\zeta y' + y = \cos\theta - 2\zeta\theta' \sin\theta \tag{20}$$

The left-hand side is the familiar linear SDOF system, but the forcing function is different. It contains a sine term from the damping element.

Again assuming a cosine argument with sinusoidally varying frequency as in Eq. (8), the EOM becomes, after the use of some trig identities,

$$y'' + 2\zeta y' + y = \cos(g\tau + h\sin p\tau) - 2\zeta g \sin(g\tau + h\sin p\tau) - \zeta ph\{\sin[(g+p)\tau + h\sin p\tau] + \sin[(g-p)\tau + h\sin p\tau]\} \tag{21}$$

Using expansions (11), the forcing function may be written as a sum of sinusoids, so that

$$y'' + 2\zeta y' + y = \sum_{m=-\infty}^{\infty} J_m(h)[\cos\Omega_m\tau - 2\zeta g\sin\Omega_m\tau - \zeta ph\sin(\Omega_m + p)\tau - \zeta ph\sin(\Omega_m - p)\tau]. \tag{22}$$

The steady-state solution can again be written as the sum of the responses to each of the harmonics present in Eq. (22):

$$y(\tau) = \sum_{m=-\infty}^{\infty} J_m(h)\left\{\frac{(1-\Omega_m^2 + 4g\zeta^2\Omega_m)\cos\Omega_m\tau + 2\zeta[\Omega_m + g(\Omega_m^2 - 1)]\sin\Omega_m\tau}{\Omega_m^4 + 2\Omega_m^2(2\zeta^2 - 1) + 1} - \frac{\zeta ph\{[1-(\Omega_m+p)^2]\sin(\Omega_m+p)\tau - 2\zeta(\Omega_m+p)\cos(\Omega_m+p)\tau\}}{(\Omega_m+p)^4 + 2(\Omega_m+p)^2(2\zeta^2-1)+1} - \frac{\zeta ph\{[1-(\Omega_m-p)^2]\sin(\Omega_m-p)\tau - 2\zeta(\Omega_m-p)\cos(\Omega_m-p)\tau\}}{(\Omega_m-p)^4 + 2(\Omega_m-p)^2(2\zeta^2-1)+1}\right\} \tag{23}$$

Exact solution (23) is cumbersome to write, but it need only be programmed once to carry out numerical studies. The mean-square response is

$$y_{\text{rms}}^2 = \tilde{J}_{-g/p}^2(h)\left\{1 + 4g^2\zeta^2 + \frac{2\zeta^2p^2h^2(1-p^2)^2 + 8\zeta^4p^4h^2}{[p^4 + 2p^2(2\zeta^2-1)+1]^2}\right\} + \frac{1}{2}\sum_{\substack{m=-\infty \\ m\neq -g/p}}^{\infty} J_m^2(h)\left\{\frac{(1-\Omega_m^2+4g\zeta^2\Omega_m)^2 + 4\zeta^2[\Omega_m + g(\Omega_m^2-1)]^2}{[\Omega_m^4 + 2\Omega_m^2(2\zeta^2-1)+1]^2} + \frac{\zeta^2p^2h^2\{[1-(\Omega_m+p)^2]^2 + 4\zeta^2(\Omega_m+p)^2\}}{[(\Omega_m+p)^4 + 2(\Omega_m+p)^2(2\zeta^2-1)+1]^2} + \frac{\zeta^2p^2h^2\{[1-(\Omega_m-p)^2]^2 + 4\zeta^2(\Omega_m-p)^2\}}{[(\Omega_m-p)^4 + 2(\Omega_m-p)^2(2\zeta^2-1)+1]^2}\right\} \tag{24}$$

Equation (24) may be used to calculate the rms response without evaluating Eq. (23) or resorting to numerical integration.

For the base motion excitation, the conditions for unbounded response are the same as for the force input: $\Omega_m \equiv g + mp = \pm 1$ ($m = 0, \pm 1, \pm 2\ldots$).

B. Parameter Studies

Parameter studies on the exact rms response (24) are now presented. The plotted value is scaled by the rms response to sine dwell base motion at the undamped natural frequency; the scaled quantity here is

$$2\sqrt{2}\sqrt{\frac{\zeta^2}{4\zeta^2+1}}y_{\text{rms}}$$

As in the previous section, the scale factor is different for each value of ζ, and the scaled response is generally higher as damping increases; the unscaled response would be lower for higher damping. The trends (Fig. 8) are nearly identical to those for the force input.

In Fig. 9, the scaled response is plotted as a function of p for fixed $h = 2$ and three values of damping. Condition (18) leads to local maxima near the values $p = 0$ and $p = 2/m$ ($m = \pm 1, \pm 2, \pm 3, \ldots$).

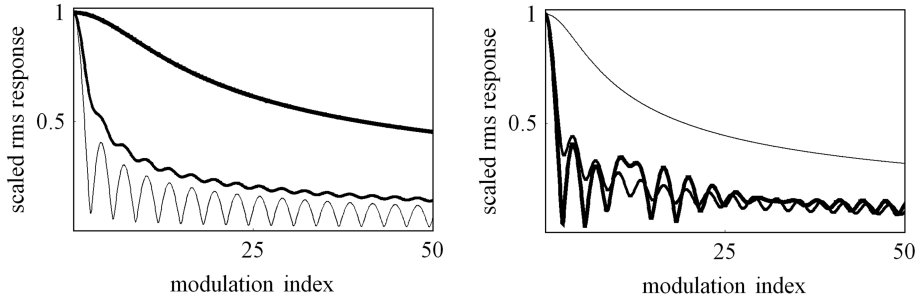

a) $\zeta = 0.001$ (thin line), $\zeta = 0.01$ (medium line), and $\zeta = 0.1$ (thick line); $g = 1$ for all curves

b) $p = 0.001$ (thin line), $p = 0.01$ (medium line), and $p = 0.1$ (thick line); $\zeta = 0.01$ for all curves

Fig. 8 Effect of the dimensionless modulation index h on the response to base motion of sinusoidally varying frequency.

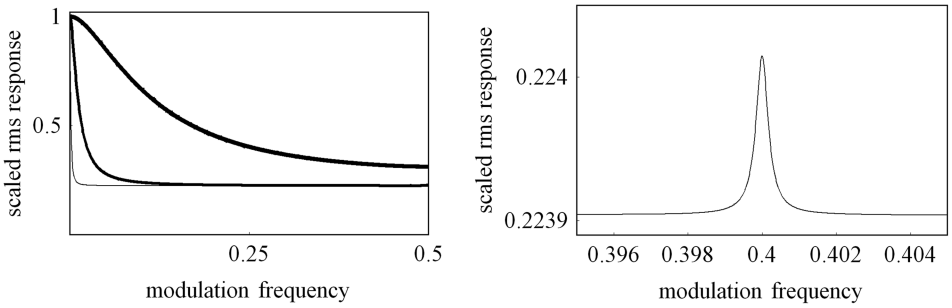

a) Response for $\zeta = 0.001$ (thin line), $\zeta = 0.01$ (medium line), and $\zeta = 0.1$ (thick line); very small local maxima exist but are not visible in this plot

b) Detail of one of the very small local maxima; only the $\zeta = 0.001$ curve is present in this plot window

Fig. 9 Effect of the dimensionless modulation frequency p on the response to base motion.

However, except for the main peak at $p = 0$, the maxima are very small. In Fig. 9, the minor peaks occur at $p = 2/4, 2/5, 2/6, \ldots$.

Next, the effect of the dimensionless center frequency g is investigated. A value of $g = 1$ indicates that the oscillating frequency is centered about the natural frequency of the excited component. Figure 10a shows the response for $p = 0.1$ and $h = 10$ and three values of ζ for g ranging from 0.8 to 1.2. For this set of parameters, a finite frequency deviation always exists, and so the response is never close to the value for sine dwell at the undamped natural frequency. Condition (18) leads to local maxima near $g = 0.8$, 0.9, 1.0, 1.1, and 1.2 in this plot. The maxima for the damped response are much more pronounced than in Fig. 9; in fact, the response is actually higher when the carrier frequency is away from the undamped natural frequency ($g = 0.9$ and 1.1) than when it equals the undamped natural frequency ($g = 1$).

Figure 10b shows the response for $\zeta = 0.01$ and $h = 10$ and three values of p for g ranging from 0.8 to 1.2. These plots show that varying frequency has a larger effect when damping is light, in agreement with previous findings [1,4]. Also, for small frequency variations, the response is greatly decreased when the center frequency is only a few percent different from the natural frequency of the excited component.

V. Rotating Unbalance with Sinusoidally Varying Speed

In previous sections, force inputs and base motions were considered. Lewis [1] intended his analysis to be applicable to rotating unbalance, but did not address the difference between his EOM and that corresponding to an unbalance excitation. Markert and Seidler [3] recognized the difference between unbalance forces and simpler excitations in the situation of linearly changing frequencies. An unbalance mass rotating at a constant speed generates a harmonic excitation of constant frequency. However, when the speed varies, the amplitude of the cosine part of the force also varies, and sine terms arise due to the tangential acceleration of the unbalance mass. In this section, the complications arising from unbalance forces are addressed for the case of sinusoidally varying frequency.

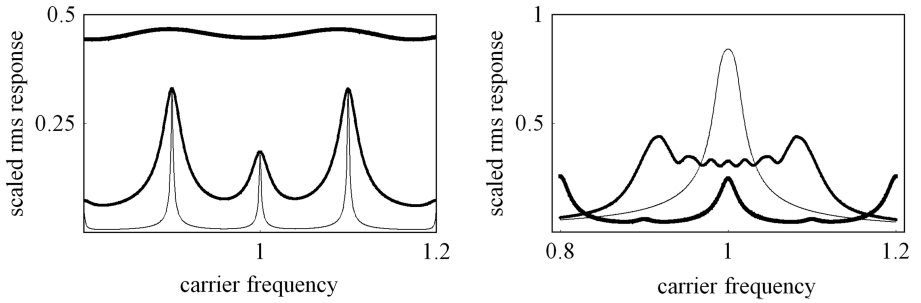

a) $\zeta = 0.001$ (thin line), $\zeta = 0.01$ (medium line), and $\zeta = 0.1$ (thick line); $h = 10$ and $p = 0.1$ for all curves

b) $p = 0.001$ (thin line), $p = 0.01$ (medium line), and $p = 0.1$ (thick line); $h = 10$ and $\zeta = 0.01$ for all curves

Fig. 10 Effect of the dimensionless carrier frequency g on the base motion response.

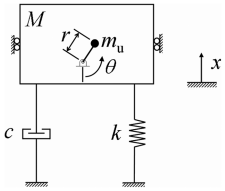

Fig. 11 Excitation of a SDOF system by a rotating unbalance.

An elementary analysis based on the mechanical model of Fig. 11, assuming the cosine argument is defined by Eq. (8) and $m_u \ll M$, shows that the EOM is

$$y'' + 2\zeta y' + y = -(g + ph\cos p\tau)^2 \cos(g\tau + h\sin p\tau) + p^2 h \sin p\tau \sin(g\tau + h\sin p\tau) \tag{25}$$

where $y \equiv Mx/m_u r$.

The forcing function contains a sine part, and both the cosine and sine parts have time-dependent amplitudes. The time dependence of the amplitudes is sinusoidal, and so one could expand the forcing function into a series of constant-amplitude sines and cosines as was done between Eqs. (9) and (12). An exact solution could be straightforwardly written down but would be extremely cumbersome.

The amplitudes of the sinusoidal parts of the amplitude variations contain the coefficients gph and p^2h^2. When the frequency changes *slowly* compared with the period of the underlying oscillations, $p \ll g$, and so these coefficients are small compared with g. Also, the time of greatest interest is often during passage through the undamped natural frequency; the constant part of the amplitude has a dimensionless value of 1 at that time. Thus, when the frequency passes slowly through the undamped natural frequency, an acceptable approximation to the actual forcing function may be obtained by omitting the sinusoidal parts of the amplitudes altogether and assigning a dimensionless amplitude of 1 to the part that is retained. This will be referred to as the "shake approximation" to the rotating unbalance force:

$$f_{SA}(\tau) = -\cos(g\tau + h\sin p\tau) \tag{26}$$

The rotating unbalance force and its shake approximation are compared in Fig. 12 for the parameter values used in Sec. III.B: $g = 1$, $p = 0.01$, and $h = 5$. For these parameter values, the forcing frequency equals the undamped system natural frequency at $\tau = \pi/2p, 3\pi/2p, \ldots = 157, 471 \ldots$. At these times, the amplitude of the unbalance force is equal to the amplitude of its shake approximation, which demonstrates the desired behavior of the shake approximation near the undamped natural frequency.

The peak response computed using the exact solution (14) for the shake approximation differs by less than 3% from the numerically computed response to the actual unbalance force, as shown in Fig. 13. Exact series solution (14) was summed through $m_{\max} = 10$ to provide an accurate estimate of the very small difference from the numerically integrated solution. The damping was $\zeta = 0.01$.

In this section, it has been shown that when the forcing frequency varies slowly through the undamped system natural frequency, the sinusoidal variations in the unbalance force amplitudes may be omitted. The important conclusion is not just that the unbalance force may be approximated by a shake, but that such an approximation allows the use of the exact solutions presented in this paper with acceptable accuracy. In other words, the solutions are *exact* for force inputs and base motions under all conditions and *inexact but acceptably accurate* for rotating unbalance when the forcing frequency passes slowly through the undamped natural frequency.

VI. Conclusions

Exact solutions for the response of a SDOF oscillator to harmonic forces and base motions of sinusoidally varying frequency have been obtained. A practical problem has been solved, and parameter studies have been presented to demonstrate the significant effects of sinusoidally varying frequency. It has been shown that the response to excitations with sinusoidally varying frequency is a strongly nonlinear function of the modulation index and modulating frequency as well as the carrier frequency and that an undamped system can have unbounded steady-state response even if the instantaneous excitation frequency never approaches the undamped

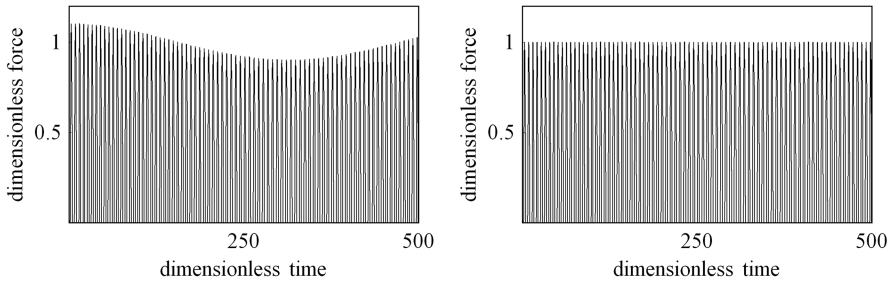

a) Exact forcing function $f(\tau)$ **b) Shake approximation $f_{SA}(\tau)$**

Fig. 12 Rotating unbalance force and its shake approximation for $g = 1$, $p = 0.01$, and $h = 5$.

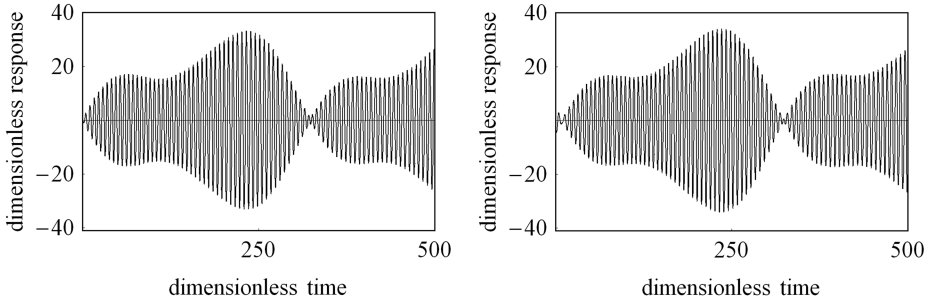

a) Response to actual rotating unbalance force, by numerical integration

b) Response to the shake approximation of the rotating unbalance force, using the exact solution

Fig. 13 Similarity of the responses to the exact input [right-hand side of Eq. (25)] and the shake-approximation input [Eq. (26)].

natural frequency. Finally, it has been shown that the exact sinusoidal-frequency solutions are accurate for rotating unbalance, provided the frequency changes slowly.

The results presented in this paper admit a broad range of excitations and therefore have many potential applications. Systems with multiple modes may be analyzed in a single modal degree of freedom when near-resonant response is of interest, provided the modes are sufficiently separated in frequency. Thus, the SDOF results presented here may be useful for more complicated, realistic systems excited by time-varying forces in a near-resonant manner. Furthermore, the time history of frequency can be written as a Fourier series, just as the time history itself can be written as a Fourier series. Exact solutions for the response to harmonic forces of arbitrarily changing frequency could be developed using the basic solution presented here for sinusoidally varying frequency.

Appendix A: Zero-Frequency Term in the RMS Response

It has been shown that the mean-square response to the force $\cos(g\tau + h \sin p\tau)$ is

$$y_{\text{rms}}^2 = \tilde{J}_{-g/p}^2(h) + \frac{1}{2} \sum_{\substack{m=-\infty \\ m \neq -g/p}}^{\infty} \frac{J_m^2(h)}{\left(1 - \Omega_m^2\right)^2 + (2\zeta\Omega_m)^2} \tag{A1}$$

where

$$\tilde{J}_m(\cdot) = \begin{cases} J_m(\cdot) & \text{if } m \text{ is an integer} \\ 0 & \text{otherwise} \end{cases} \tag{A2}$$

The zero-frequency term represented by $\tilde{J}_{-g/p}^2(h)$ occurs only when g/p is an integer and is only significant for small values of that integer. Consider the case $g = 1$, $p = 1$, and $h = 2$. This forcing function is plotted in Fig. A1a. For damping of $\zeta = 0.01$, the mean-square response for this near-resonant condition, from Eq. (A1), is 218, of which 0.333 comes from the zero-frequency term, a negligible contribution.

Now consider the case $g = 2$, $p = 2$, and $h = 2$. This forcing function is plotted in Fig. A1b. This is not a near-resonant condition, and the mean-square response is only 0.343. But now the 0.333 contributed by the zero-frequency term is a significant part of the total response.

Because the zero-frequency term appears only when g/p is exactly integral, the function $y_{\text{rms}}(g)$ has discontinuities. The discontinuities may be explained by considering the time history of the response rather than just the mean square.

Again, assume $p = 2$, $h = 2$, and $\zeta = 0.01$. Consider $g = 1.9990$, which is very near, but not exactly, the value $g = 2$ for which the zero-frequency term exists. The steady-state response, calculated from Eq. (14), oscillates within an oscillating band centered on zero, as shown in Fig. A2a. As g approaches 2, the envelope oscillates with a longer and longer period (Fig. A2b, for $g = 1.9999$), still about a mean of zero. Then for $g = 2$, the period of the envelope becomes infinite (Fig. A2c). (The oscillations are too rapid to be discernible in these plots; the thick stripe represents the envelope.) The response oscillates within a fixed band about a negative mean. Because the mean square of a function is defined in terms of its limiting behavior over an infinite time period, the mean-square response jumps exactly for the value of g at which the period of the envelope becomes infinite, because the response is no longer centered about zero. The discontinuous zero-frequency term accounts for this sudden jump in the rms response. For any value of g other than exactly 2, the envelope's period is finite, giving the response a different character with respect to its mean behavior.

It is tempting to discard the zero-frequency term on the grounds that for a physical forcing function, g could not be *exactly* an integral multiple of p for longer than an instant. However, similar reasoning could be applied to any term in the sum, because every component of the response is associated with a discrete frequency. A stronger argument for discarding the zero-frequency term is to note that for most problems of practical interest, g/p is large compared with h.

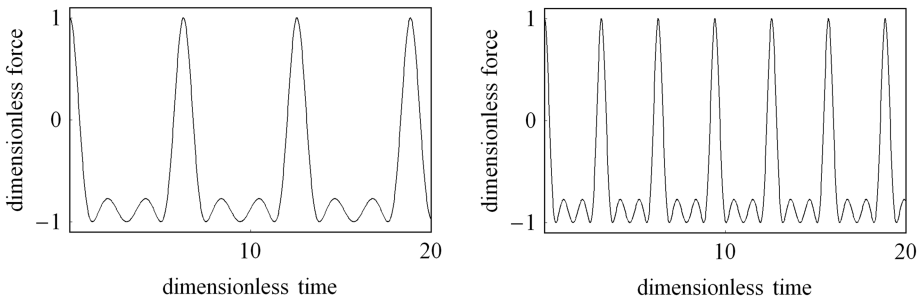

a) With $g = 1$ and $p = 1$; the dimensionless mean square response to this forcing function for $\zeta = 0.01$ is 218

b) With $g = 2$ and $p = 2$; the dimensionless mean square response to this forcing function for $\zeta = 0.01$ is 0.343

Fig. A1 Forcing function (8) for two different sets of parameters.

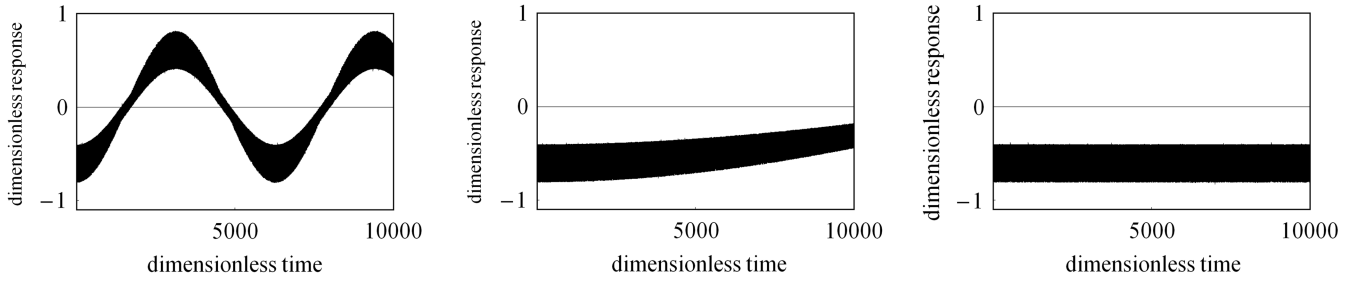

a) Response for $g = 1.9990$

b) Response for $g = 1.9999$

c) Response for $g = 2.0000$

Fig. A2 Behavior of the response for values of the carrier frequency g very near the value $g = 2$ at which the zero-frequency term appears in the rms response. The underlying oscillations are too rapid to be discernible; the thick stripe shows the response envelope.

Referring to the Bessel function plots in Fig. 3, the zero-frequency term practically vanishes in such cases.

Acknowledgments

The author thanks E. K. Hall and A. M. Kabe of The Aerospace Corporation and A. E. Semple of Analex Corporation for valuable comments. This work was carried out for the U. S. Air Force, Space and Missile Systems Center, Los Angeles Air Force Base, California.

References

[1] Lewis, F. M., "Vibration During Acceleration Through a Critical Speed," *Transactions of the ASME*, Vol. 54, No. 1, 1932, pp. 253–261.

[2] Zhou, S., and Shi, J., "The Analytical Imbalance Response of Jeffcott Rotor During Acceleration," *Journal of Manufacturing Science and Engineering*, Vol. 123, No. 2, 2001, pp. 299–302. doi:10.1115/1.1352021

[3] Markert, R., and Seidler, M., "Analytically Based Estimation of the Maximum Amplitude During Passage Through Resonance," *International Journal of Solids and Structures*, Vol. 38, Nos. 10–13, 2001, pp. 1975–1992. doi:10.1016/S0020-7683(00)00147-5

[4] Cronin, D. L., "Response of Linear, Viscous Damped Systems to Excitations Having Time-Varying Frequency," Ph.D. Thesis, California Inst. of Technology, Pasadena, CA, Aug. 1965.

[5] Hindmarsh, A. C., "ODEPACK, A Systematized Collection of ODE Solvers," *IMACS Transactions on Scientific Computation*, North-Holland, Amsterdam, Vol. 1, 1983, pp. 55–64.

[6] Sturley, K. R., *Frequency Modulation*, Chemical Publishing Company, Brooklyn, NY, 1950.

[7] Cantrell, C. D., *Modern Mathematical Methods for Physicists and Engineers*, Cambridge Univ. Press, New York, 2000.

R. Kapania
Associate Editor